Vol. 44, No. 2 (2022) 253-267, DOI: 10.24874/ti.1131.06.21.08

Tribology in Industry

www.tribology.rs

RESEARCH

Optimization of Abrasive Wear Parameters of Halloysite Nanotubes Reinforced Silk/Basalt Hybrid Epoxy Composites using Taguchi Approach

S.M. Darshan[a,b], Bheemappa Suresha[a,*], Imran M. Jamadar[a]

[a]*Centre for Composite Material Research, Department of Mechanical Engineering, The National Institute of Engineering, Mysuru-570008, Karnataka, India,*
[b]*Department of Mechanical Engineering, CHRIST (Deemed to be University), Bengaluru-570008, Karnataka, India.*

Keywords:

Silk fibre
Basalt fibre
HNTs
Hybrid nanocomposites
Three body abrasive wear
Taguchi method

* Corresponding author:

Bheemappa Suresha
E-mail: sureshab@nie.ac.in

Received: 10 June 2021
Revised: 2 August 2021
Accepted: 29 August 2021

A B S T R A C T

The demand for environmentally friendly and sustainable materials for nonstructural and structural applications grows by the day. Polymeric composites reinforced with fillers and fibres are considered to have increased strength and desirable wear resistance. Abrasive wear of industrial and agricultural based components are currently one of the most serious issue. Therefore, the current research reports on the influence of Halloysite-Nanotubes (HNTs) loading on the three body abrasive behavior of bi-directional silk fibre (SF) and basalt fibre (BF) reinforced epoxy (Ep) composites. Rubber wheel with dry sand abrasion testing in accordance with ASTM G65-16e1 was performed with four control parameters such as filler content, load, abrading distance and silica sand size. The tests were planned as per orthogonal array of Taguchi (L_{27}). Significant impact of control factors were identified using ANOVA (Analysis of variance). The results demonstrated that adding HNTs to SF-BF/Ep nanocomposites significantly improved the wear resistance and the combination of A_2, B_1, C_3 and D_1 control factors yields the lower specific wear rate (SWR). Findings exhibit that the load and abrading distance were the most significant parameters affecting the abrasive wear of SF-BF/Ep nanocomposites followed by filler content and silica sand size. Microstructural features were observed via scanning-electron-microscopy (SEM).

1. INTRODUCTION

Fibre reinforced polymeric composites (FRPCs) have seen exponential growth over the last few decades, with its increased usage in various engineering components and structures owing to unique properties like higher specific modulus, efficiency, strength to weight ratios, resistance to environmental degradation, exceptional processability, and economic viability [1,2]. The matrix or fibre alone cannot accomplish the properties of FRPCs. The fibre-matrix interactions has a considerable impact on composite performance. Although interfacial

knowledge has been acquired for many synthetic FRPCs, it is still not fully recognized for natural fibre reinforced composites. The scientific emphasis has shifted from mono-FRPCs to natural-synthetic fibre FRPCs [3,4]. Particulate filled polymeric composites have gained popularity owing to their widespread applications. The tribological behavior of particulate reinforced polymeric composites are highly influenced by its shape, size and dispersion of the fillers along with the increased adhesion at its interface [5]. Polymeric composites are frequently expected to come into contact with its hard abrasives as a counterface. The market for novel materials that can work in mechanical components attributed to relative motion without the use of lubricant is constantly growing. It has intensified the industrial development of newer material systems, such as bearing parts in the automobile sector. Another advantage is that they have a low frictional coefficient, particularly in some specifically engineered systems [6].

Due to many benefits like widespread availability, low weight, lower emission of CO_2, recyclability and biodegradability, composites reinforced with natural fibres have seen an increased usage in recent years [7]. Silk fibres consist mostly of fibroin which is protein based at its inner-layer and sericin as outer layer, which is spun off by cocoons [8]. Silk constitutes a chemical composition of 17-25% sericin, 75-83% silk-fibroin and 2.5% of other ingredients. Silk-fibres have been selectively hybridized with polymeric materials because of the ability of silk fibres to enhance the load bearing capabilities and decelerate crack propagation, but the tribological study is rarely reported [9,10]. Natural fibres performs an important role in tackling contemporary environmental challenges during the development of FRPCs. They are lightweight, but have poor mechanical characteristics when compared to synthetic fibres. This problem can be solved by using hybrid fibres, which combine artificial and natural fibres. The majority of natural fibre literature focuses on mono-fibre reinforcement. Hybridization could be a best possible solution to the cost- effective fulfilment of different and competitive design requirements relative to conventional engineering materials [11,12].

Due to their chemical and physical properties, the basalt found in volcanic rocks may be a good pick for polymeric composites. It is similar to a chemical composition of glass, with main components being K_2O SiO_2, MgO, Na_2O CaO, Na_2O, Fe_2O_3, Al_2O_3 and FeO [13]. Park et al. [14] discussed their improved interfacial properties of basalt hybridization. On the basis of a literary survey on the efficient usage of basalt fibre as a reinforcement in different polymers there was limited evidence. The hybridization and the synergic effect of silk fibres and basalt fibres are expected to escalate the scope of hybridized polymer composites.

Nanofillers are incorporated to improve the properties of biocomposites and are usually added into polymer matrices of 1% to 5% by weight. HNTs are made of naturally deposited aluminum silicates ($Al_2Si_2O_5(OH)_4H_2O$) and are chemically similar to kaolin. Given that the tubular framework is hollow in nature, it allows HNTs to have a high aspect ratio that makes extraordinary matrix and filler interaction possible resulting in improved mechanical characteristics [15]. Epoxy is used as a matrix material and is one of the most widely used polymer with many advantageous properties such as strong adherence, high strength, efficient load transfer, and indentation resistance, but brittleness and low epoxy fracture toughness, costing its application [16]. Therefore, much work has been done and increase in the properties of polymeric composites were observed with the incorporation of fillers at nano level due to the effective load transfer mechanisms and increase in cross link densities [17,18]. Composite systems are comparatively cheaper, eco-friendly and easier to use when bio-fibres are reinforced in synthetic fibres [19]. The best way of achieving cost-effective compliance with the various and competitive design criteria in respect of traditional engineering materials may be hybridization [20]. As effective reinforcement in hybrid composites, a novel combination of silk, basalt fibres and HNTs are chosen for its beneficial synergetic effects in increasing the specific strength and ecological impacts of several other synthetic fibre reinforced composites.

Wear is characterized as the progressive removal of materials from a solid surface caused by the relative movement of the surface

with its contacting substance [21]. The leading source of wear in the industry is by abrasion, contributing almost 63% of the total cost for wear. Wedge-formation, ploughing and microcutting are the main mechanisms in which wear by abrasive occurs. Abrasion wear rate is governed by a wide range of variables, including operational conditions, parameters of design, abrasion characteristics and properties of material. The abrasion condition can occur in different machines, for example in the vanes, gears, sewers, coke-coated jackets, bushes and seals, equipment's used for mining [22,23]. Abrasive wear occurs mainly in two forms, namely three-body and two-body abrasion. Hard and rough surface slide through the softer surface resulting in the removal of material in two body abrasion, while three-body abrasion is caused by the slipping and rolling of harder particles entrapped in between the sliding surfaces. Most of the material removal processes in agricultural products and engineering structures occur by three body abrasion [24]. Yousif et al. [25] employed betel-nut fibre to improve the wear resistivity of unsaturated polyesters. The addition of nano-TiO_2 reduced the wear loss in FRPCs [26]. Shao et al. [27] fabricated TiO_2-SiO_2 filled epoxy composites displayed enhanced resistance to wear as compared with the unfilled ones.

Three body abrasive wear (3BAW) is commonly regarded as more realistic; however, it seems to have gained fewer focus than a problem with two-body. Some research on polymeric composites that are susceptible to the abrasive wear has been published in the recent years [28]. The effect of different loading of fillers on the abrasive wear properties of basalt/epoxy composite was examined by Sahin et al. [29]. Improved resistance to 3BAW was observed with the incorporation of nanoclay to basalt/epoxy composites [30]. Patnaik et al. [31] investigated several particles such as Al_2O_3, SiC, and pine bark dust and concluded that the particles loaded composite had the highest wear resistance. Namdeo et al. [32] shown that the addition of organically modified montmorillonite improved tribological characteristics of composites. The 3BAW behaviour of basalt fibre reinforced hybrid epoxy composites were examined by Sharma et al. [33]. Suresha et al. examined the abrasion wear properties of vinyl-ester/epoxy composites reinforced with different fabrics and particulate fillers [34-36]. ANOVA and Taguchi's orthogonal design was deployed to determine the influence of individual process-parameters. The 3BAW characteristics of a polyester based hybrid composites reinforced with natural and synthetic fibers was studied by Sakthivel et al. [37]. Subbayya et al. [38] used the L_{27} Taguchi orthogonal design, which demonstrated that the load and abrading distance had a greater significance and percentage contribution when considered individually than considering in combinations. Ramesh and Suresha [39] used Taguchi design and ANOVA, and described how load and filler loading impacts the abrasion. They also analysed the relationship between sliding and abrasion wear. The optimization of 3BAW parameters such as load, abrading distance and filler content of HNT filled composites using L_{16} array was demonstrated by Muralidhara et al. [36]. Many tribologists have investigated the effect of nanoparticles on the tribological behaviour of epoxy based composites [30,36,40].

The novelty of this work is the development of wear resistant bio-friendly polymer composites. The scientific community has yet to attempt the novel concept of selecting HNTs for the tribological characterisation of SF-BF/Ep composites. The current research explores the wear behaviour of HNTs filled SF-BF/Ep composites subjected to three body abrasion. The majority of studies has focused on extensive experimental works with the impact of one parameter while retaining all remaining factors constant. However, this method is not recommended since in the practical situations there exists a combination of interacting factors affecting abrasive wear. As a result, in the current analysis, an effort is made to investigate the influence of different interacting factors in addition to the main effects. To accomplish this, Taguchi's design of experiments (DOE) is deployed. Konishi and Taguchi are advocates of this approach [41]. Taguchi method utilizes orthogonal arrays with special design to analyse the complete parameter space only with a few experiments. The technique of Taguchi also helps to optimize the vital parameters [42]. In addition, the ANOVA test was run on the experimental data to determine the most important factors influencing the SWR.

2. EXPERIMENTAL PROCEDURE

2.1 Materials

Halloysite nanotubes (HNTs) with lengths of 10-15 μm and diameters of 30-70 nm were obtained from the Sigma-Aldrich Company in Bengaluru. HNTs consist of tubular structures with approximately 70 $m^2.g^{-1}$ surface area and a 2.53 $g.cm^{-3}$ density. This has a lower percolation properties and higher aspect ratio, rendering it convenient for its usage as reinforcement in epoxy matrix. Siera Mills Pvt. Limited in Bengaluru supplied the silk fibres. In the current research, we have used plain bi-directional woven silk and basalt fibres of 70 GSM and 200 GSM respectively (Fig. 1). Huntsman Advanced Materials India Pvt. Ltd., Mumbai, provided the epoxy (LY556) and hardener (HY951). Table 1 and 2 represents the properties of the ingredients used for the nanocomposites.

Table 1. Properties of the fibre and the matrix.

Properties	Silk fiber	Basalt fiber	Epoxy
Density (g/cm^3)	1.3	2.67	1.2
Tensile strength (MPa)	500	2800	50
Tensile modulus (GPa)	8.5	89	2.8

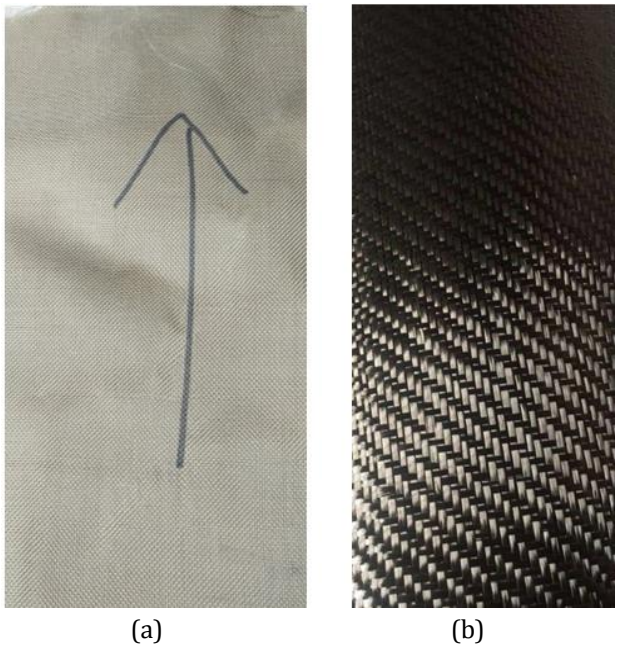

(a) (b)

Fig. 1. Bi-directional woven fabrics: (a) silk (b) basalt.

Table 2. Properties of the HNTs.

Form	Nano-HNTs
Density	2.53 g/cm^3
Diameter	30-70 nm
Length	10-15 μm
Surface area	$64m^2/g$

2.2 Nanocomposite fabrication

Hybrid nanocomposites were fabricated according to the standard procedures following a detailed literature study with vacuum bagging process. To ensure a uniform dispersion and better intermolecular interactions, HNTs were blended with the epoxy using an ultrasonicator. A small amount of HNTs was slowly dispersed in the epoxy resin solution and sonicated for 1 hr (Fig. 2). Degassing is done for about 30 min in a vacuum oven at 100 ^{0}C to remove any air bubbles that may have formed in the resin mixture. Hardener is introduced to the epoxy at a ratio of 1:10. The silk fabrics are stacked one over another with basalt fabrics at equidistance's, and the nano-resin mixture is distributed well between silk and basalt fabrics for obtaining hybrid nanocomposites using vacuum bagging method (Fig. 3). Uncured nanocomposite laminates were kept over 48 hrs before final curing at a room temperature of 24 ^{0}C.

Schematic depiction of the fabrication procedure for HNTs filled hybrid nanocomposites is represented (Fig. 4). The fabricated laminate has dimensions of 300 mm × 300 mm × 3 mm. Table 3 describes the descriptions of the hybrid nanocomposites.

Table 3. Composition and designation of hybrid SF-BF/Ep nanocomposites.

Designation	Composition
SF-BF/Ep	Epoxy (50 wt. %) + Basalt fiber (25 wt. %) + Silk fiber (25 wt. %)
SF-BF/Ep-1.5HNT	Epoxy (48.5 wt. %) + Basalt fiber (25 wt. %) + Silk fiber (25 wt. %) + HNT (1.5 wt. %)
SF-BF/Ep-3HNT	Epoxy (47 wt. %) + Basalt fiber (25 wt. %) + Silk fiber (25 wt. %) + HNT (3 wt. %)

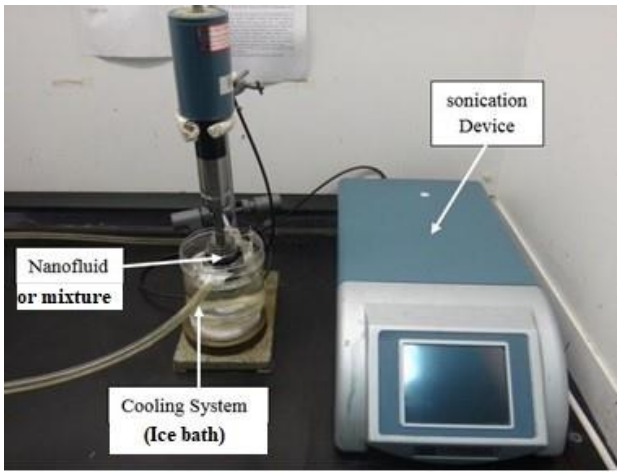

Fig. 2. Sonicator setup.

Fig. 3. Vacuum bagging process.

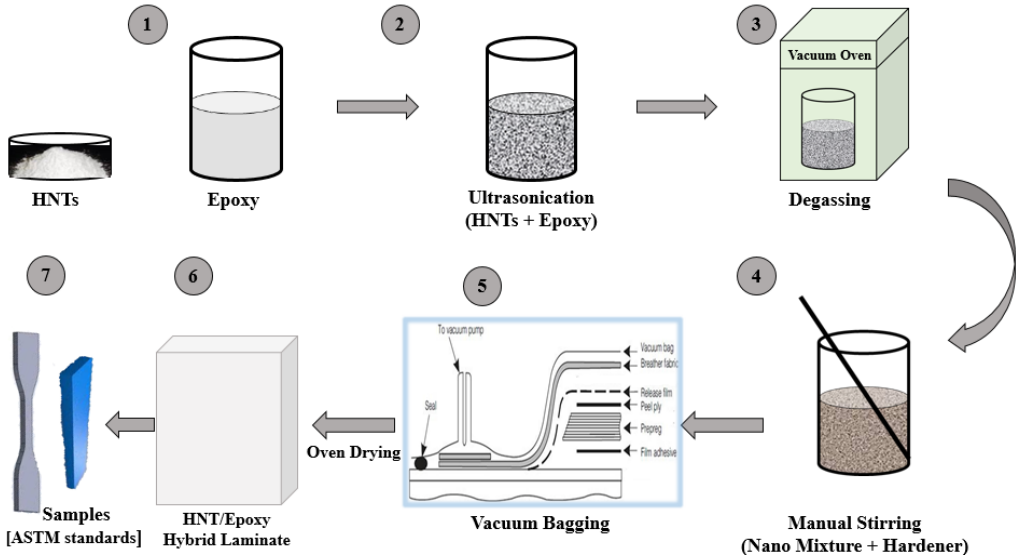

Fig. 4. Schematic representation of fabrication process of HNTs filled hybrid nanocomposites.

2.3 Three-body abrasive wear test

Three body abrasion wear investigations were performed using a rubber wheel/dry-sand wear test setup from Magnum engineers, Bengaluru as per ASTM-G65-16e1 standard (Fig. 5). Before and after the test, sample surfaces have been cleaned thoroughly with acetone. Prior to mounting the samples in the specimen holder, the samples weight were recorded by means of an electronic digital balance (with accuracy of 0.1 mg). Table 4 represents the specifications of 3BAW tester. There were at least three experiments for each material configuration to ensure that the test results could be replicated and the mean values are reported. The wheel rotations are such that it's contacting surface moves freely with the grit flow. Lever arm's pivotal axis lies in a plane which is roughly normal to its horizontal diameter and tangent to surface of rubber wheel.

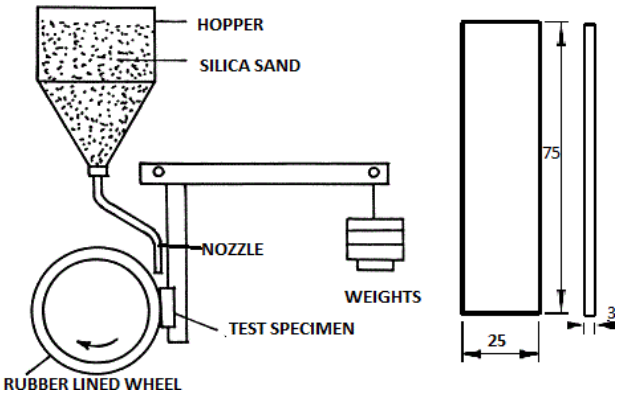

Fig. 5. Schematic illustration of rubber wheel/dry sand abrasion tester.

The test runs were done with a constant speed-200 rpm. The abrasive particles were fed at a rate of 225±10 g/min. SWR (K_S) was determined using equation 1.

$$K_S = \frac{\Delta V}{Ld} \frac{mm^3}{Nm} \quad (1)$$

Where ΔV denotes volume loss, L denotes load, and d denotes abrading distance.

Table 4. Three body abrasive wear technical specifications.

Parameters	Testing conditions
Diameter of rubber wheel	228.6 mm
Rotational speed of rubber wheel	200 rpm
Sand flow rate	225 ± 10 g/m.

2.4 Experimental design

Taguchi's DOE has been used to reduce the number of test runs and determine the optimal composite composition (Fig. 6). This approach is commonly used for optimization of the quality characteristic for a combinations of various input parameters. Minitab 19 software is used to perform experimental runs using such a strong analysis tool. Table 5 displays control factors and their levels that would affect the response performance in Taguchi's system. In order to have better study of the quality characteristics and to develop a more accurate regression equation it is required to have more data points for fitting the model. Hence L_{27} array is adopted in the present work for the four variables and three levels. Three kinds of quality loss function have been obtained in Signal to Noise analysis (S/N): nominal the better; higher is the better; lower the better. Thus, the lower the better function was used to obtain the optimum wear-rate parameters.

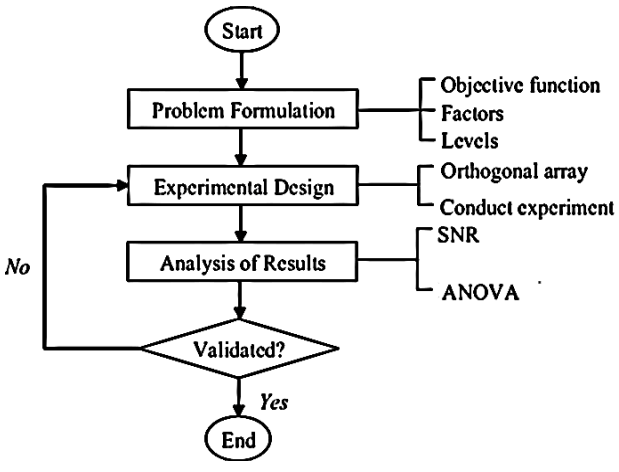

Fig. 6. Flow chart of Taguchi optimization method.

Table 5. Control factors and their levels.

Level	Filler Content (%)	Load (N)	Abrading distance (m)	Silica sand size (μm)
1	0	20	250	225
2	1.5	30	500	325
3	3	40	750	425

2.5 Microstructure and worn out surface analysis

The microstructure of the silk, basalt fabric (plain weave), HNT filler and the worn out surfaces were examined using scanning electron microscopy (Quanta-200 model, FEI-Netherland make) with operational voltage of 20 kV. Specimens were fixed on to carbon tape on aluminium stubs and then sputter coated with gold to make them conductive prior to SEM observation.

3. RESULTS AND DISCUSSIONS

3.1 Microstructure of HNT filled hybrid composites

SEM photographs representing basalt and silk microstructure (Fig. 7a and 7b) demonstrates a densely woven fabric in orthogonal directions without any porosity between the fibres. Basalt and silk fabrics have a density (areal) of 200 GSM and 70 GSM respectively, providing the hybrid composites with a higher density of packing.

The orientation of fibre was reported to have substantial influence on its compaction properties of fibre reinforced composites. The triangular forms of a silk fibres (Bombyx-mori) with concave and convex cross-sections will allow improved and better "intra-yarn" packing density relative to polygonal and irregular sections of other bio based fibres [43]. With vacuum moulding, fibre reinforcement loadings of up to 50 wt. % were achieved. Our research substantiates claims of enhanced fabric compaction properties. SEM images of HNTs (Fig. 7c), which exist in tubular shape with diameters varying from 30 to 70 nm and length varying from 1 to 15 μm.

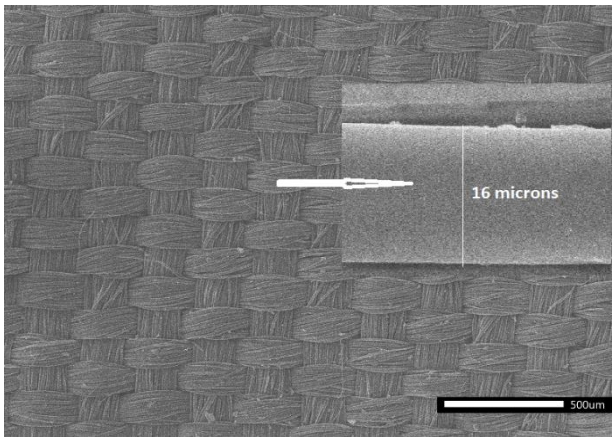

(a)

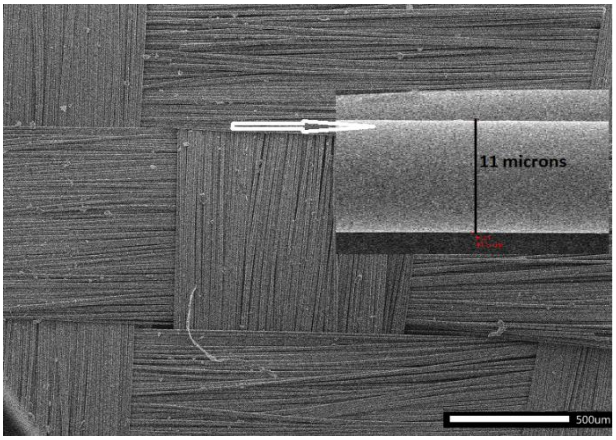

(b)

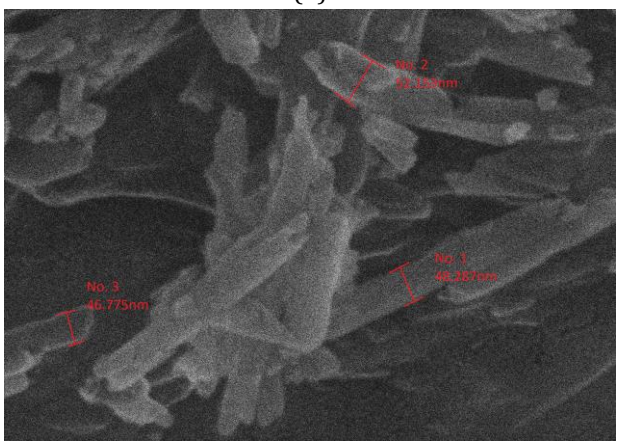

(c)

Fig. 7. Microstructure of (a) Silk fabric, (b) Basalt fabric, (c) HNTs.

The uniform distribution of the composite's ingredients improves the material characteristics. In this regard, the SF-BF/Ep composite was analyzed for the proper dispersion of HNTs. To analyze the dispersion of the constituents, the element mapping with the help of energy dispersive analysis of X-rays (EDAX) has been done (Fig. 8). The elemental mapping of oxygen, silicon and aluminum are represented (Fig. 8b–d).

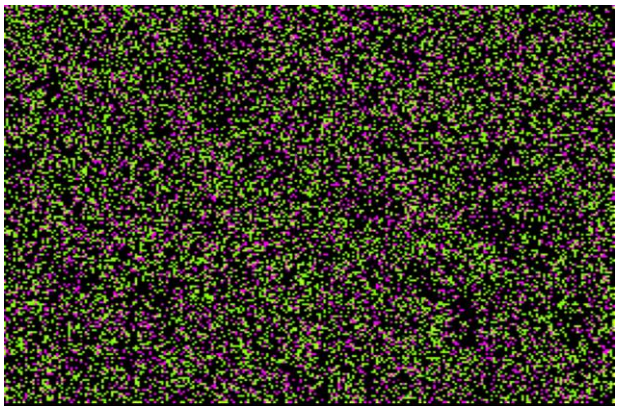

(a)

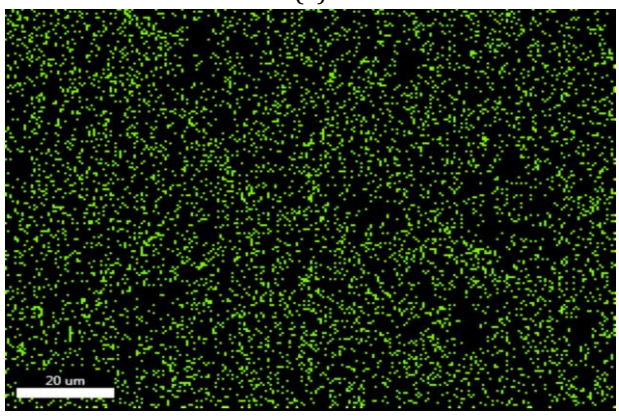

(b)

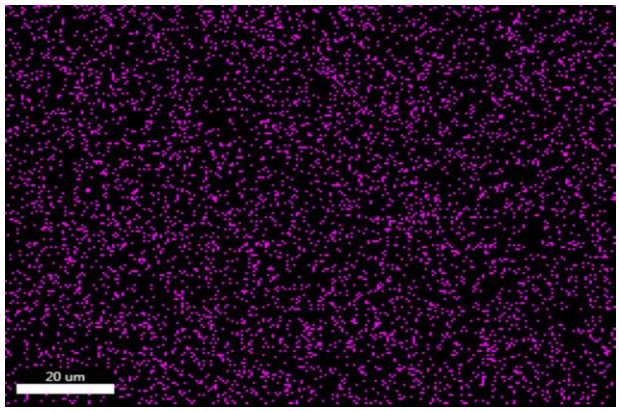

(c)

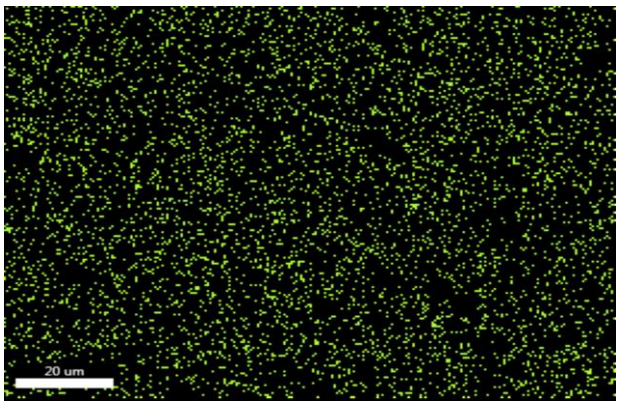

(d)

Fig. 8. Mapping of the hybrid nanocomposites using EDAX (a) Total elemental overlay (b) Oxygen (c) Aluminium (d) Silicon.

The density of the aluminum and silicon is high and the higher density can be attributed to the presence of HNTs. However, the density of carbon and other constituents are relatively lesser. The oxygen is present in the polymer chains of polymer, silk and basalt fabric. The nitrogen can be traced only in the polymer chain, hence the element density is still lesser when compared to that of oxygen. The uniformity in the aluminum and silicon mapping can be taken as a witness to validate the good dispersion. Bijwe et al. have employed the similar procedure to analyze the element mapping of wear surface [44].

3.2 Statistical analysis of wear

The HNTs reinforced SF-BF/Ep nanocomposites' abrasive behaviour subjected to three body mode is studied based on the filler content, load, abrading-distance and silica sand size. The L_{27} array of Taguchi's experimental design is simulated. Table 6 lists the experimental SWR and the corresponding S/N ratio.

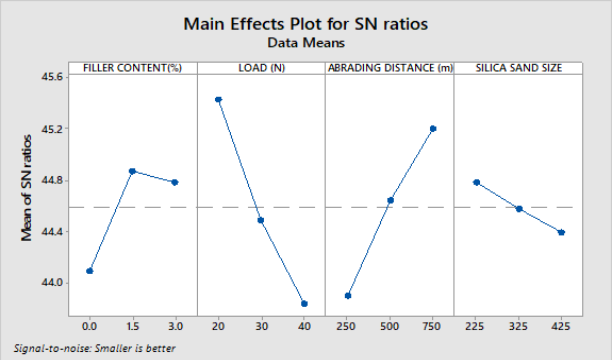

Fig. 9. Influence of control factors on the S/N ratio

Table 6. L_{27} orthogonal design and the performance results.

SL NO.	FILLER CONTENT (%)	LOAD (N)	ABRADING DISTANCE m)	SILICA SAND SIZE (µm)	SWR (mm³/Nm)	S/N Ratio (dB)
1	0	20	250	225	0.0060234	44.4032
2	0	20	500	325	0.0056491	44.9604
3	0	20	750	425	0.0053743	45.3936
4	0	30	250	325	0.0068496	43.2867
5	0	30	500	425	0.0063742	43.9115
6	0	30	750	225	0.0057248	44.8448
7	0	40	250	425	0.0074744	42.5285
8	0	40	500	225	0.0066249	43.5764
9	0	40	750	325	0.0063495	43.9452
10	1.5	20	250	325	0.0055997	45.0367
11	1.5	20	500	425	0.0053246	45.4743
12	1.5	20	750	225	0.0046743	46.6057
13	1.5	30	250	425	0.0063247	43.9792
14	1.5	30	500	225	0.0055745	45.0759
15	1.5	30	750	325	0.0053997	45.3526
16	1.5	40	250	225	0.0065742	43.6431
17	1.5	40	500	325	0.0061991	44.1534
18	1.5	40	750	425	0.0059244	44.5471
19	3	20	250	425	0.0057919	44.7436
20	3	20	500	225	0.0050311	45.9667
21	3	20	750	325	0.0048563	46.2739
22	3	30	250	225	0.0062315	44.1081
23	3	30	500	325	0.005756	44.7976
24	3	30	750	425	0.0055912	45.0499
25	3	40	250	325	0.0067566	43.4054
26	3	40	500	425	0.0063814	43.9017
27	3	40	750	225	0.0057317	44.8343

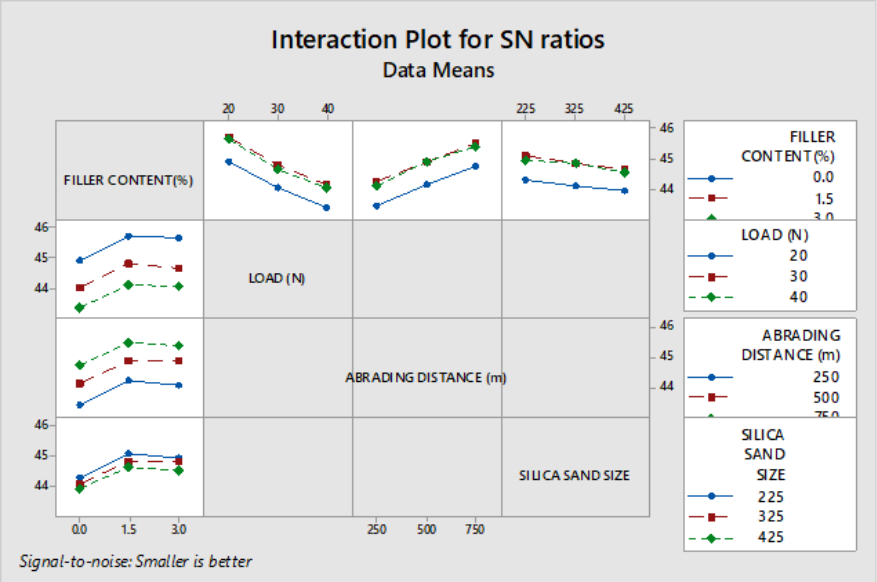

Fig. 10. Intersection plot for SN ratios.

The mean S/N ratios for experiments conducted for the HNTs filled SF-BF/Ep nanocomposites under study was 44.59 dB. The influence on the SWR by the control factors are shown graphically (Fig. 9 and 10). Setting of controlling factors with the largest S/N ratio consistently resulted in its optimum output with the least variance. Transition of S/N ratio as control factor setting was shifted from its one level to its next is displayed (Fig. 9). The optimal SWR in the response graphs was the larger S/N value [45,46]. The graph shows that combining control factor of A_2, B_1, C_3 and D_1 gives the lower SWR. The optimal parameter setting responsible for the minimum SWR are filler content at level 2, load and silica sand size at level 1, abrading distance at level 3 i.e, the developed polymeric nanocomposite have the lowest SWR when the load and silica sand size are at their lowest level, and the abrading distance is at its highest level. That might be owing to the reasons that the HNTs in the composites as fillers tends to slip in the abrasion phase, leading to reduced SWR.

The SN ratios declines with the increase in load and silica sand sizes, increases with increase in abrading distance for all materials, but partially rises with the filler content. Amongst the variables, the load is the most significant factor in determining materials' wear resistance. The results range from 42.528 dB to 46.606 dB. The SN ratio is initially very high for load and gradually declines. At lower loads, the energy induced by abrasive particles is insufficient to break the energy barrier of surface formed at the interface of the abrasive particle and test specimen, preventing abrasive particles from penetrating deeper into matrix material; however, at higher loads, particles acquire energy from rubber wheel rotating at higher speed, resulting in high SWR (Lower SN ratio). When fillers are added to the composite, the energy barrier increased. The energy gained from the rubber wheels rotation is sufficient for micro-cutting a significant number of fibers. Load is followed by the abrading distance, filler content and silica sand size. The SWR reduces as the abrading distance increases from 250 m to 750 m. Previous researchers noticed a similar trend [36,46]. As a result, for all of the investigated materials, the response is highly dependent on the applied load and abrading distance. Load had a greater influence on the wear behavior of PTFE composites than the other control parameters [47]. The SN ratios decreased, when tested against 225 to 425 μm grit due to increase in the sample's penetration ability. Furthermore, filler content and bonding in between particle and polymer appear to be important for wear reduction. For instance, existence of strong bonding between matrix and filler, separation of the sample surface becomes more difficult, contributing to higher wear resistance. The poor bonding in between the filler and the polymer matrix probably results in a significant reduction in wear resistance, because the particles are easily detached from the polymer during 3BAW at their contact zone [48].

Table 7 shows the S/N ratio response. The S/N ratio delta values of filler content, load, abrading distance and silica sand size are 0.78, 1.59, 1.3 and 0.39, respectively. The most significant effect on the SWR was by load, followed by abrading distance, filler content and silica sand size.

Table 7. Response data for S/N ratios under three-body abrasion.

Level	FILLER CONTENT (%)	LOAD (N)	ABRADIND DISTANCE (m)	SILICA SAND SIZE (μm)
1	44.09	45.43	43.9	44.78
2	44.87	44.49	44.65	44.58
3	44.79	43.84	45.21	44.39
Delta	0.78	1.59	1.3	0.39
Rank	3	1	2	4

Interaction effects on S/N ratios by the process parameters are represented graphically (Fig. 10). The smaller the better quality characteristics were chosen to optimize the SWR. Interactions will not occurs whenever the interaction lines are parallel and when lines are crossed, strong interactions among control factors occur. The minimum wear rate is assured from the process parameters with optimal setting of $A_2B_1C_3D_1$ and same needs to be evaluated experimentally. The first row has three plots. The first plot is the variation of the SN ratio with load, and the second plot is a variation of SN ratios with abrading distance, the third plot is the variation of SN ratios with silica sand size for each loading condition. This gives the interaction of the three control factors (load, abrading distance and silica sand size) by keeping one control factor (filler content) as a varying parameter. From the first row graph, it is worth noting that for any filler content; the SN ratio is higher for 20 N, 750 m abrading distance and 225 μm silica sand size. Similarly, in the second, third and fourth row represents the variation of SN ratios with filler content was addressed for the different loads, abrading distances and silica sand sizes respectively with the highest SN response for 1.5 wt. % of HNTs. Though the number of the experiments was reduced to 27, the overall variations were predicted and plotted in these interaction plots. Statistical study (ANOVA) was carried out to justify the interactions.

3.3 ANOVA and effect of various control factors

ANOVA is the tool deployed to statistically design the individual effects of all control variables. Table 8 illustrate the findings of the ANOVA study. To calculate the corresponding impact of process parameters on quality characteristics, percentage contribution of every factor has been considered. This study was executed with a significance level of 5%, and with 95% for confidence. Last column in Table 5 represents the level of importance between process parameters and interactions, percentage contribution of every factor on overall variance which indicates the influence of the parameters on wear. When the ANOVA for the three body wear results of HNTs reinforced silk/basalt composites was examined, the main factor contributing to SWR was the load preceded by the abrading distance.

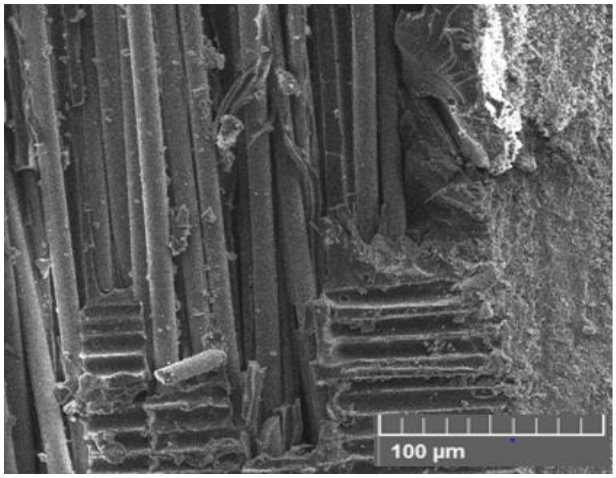

(a)

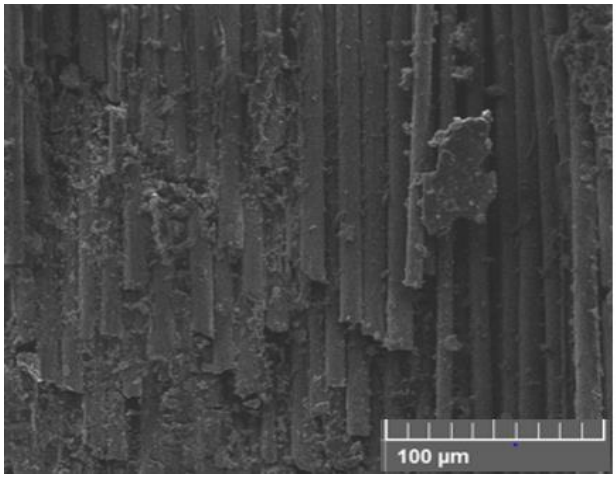

(b)

Fig. 11. SEM micrograph of abraded surface (a) SF-BF/Ep (b) SF-BF/Ep-1.5HNT composites.

Table 5 illustrates the importance of control factor- Load has larger influence of 49.58% followed by abrading distance-33.02%, filler content-14.14% and silica sand size-2.98% on SWR of the hybrid nanocomposites under analysis. This method assigns the variation of variance and means to the absolute values which are considered and measured during the experiment rather than the variable's unit value. Interaction of the parameters therefore has an effect of <1 %, and the contribution to SWR is less significant [49]. The load is more significant, which could increase abrasion of the polymer composite. The ploughing action of the abrasive medium will be lesser at lower loads which will result in lower SWR and vice versa and same is reflected in ANOVA. Also at higher abrading distance, the broken HNT particles will also be acting as third body which will result into increased roughening of the counter surface, leading to increased wear loss.

Within the experimental conditions, the applied loads in this study are sufficient to induce stress at the contact region. The abrasive particles during three-body abrasive wear are initially free flowing and come in contact with other two surfaces (specimen and the rubber wheel). The abrasive particles' irregular form allows them to behave like a ploughing agent [50]. The grooves were created since the matrix material was continuously removed from the specimen's surface. The micro-cutting effect on the high-modulus fibres is performed after removing the matrix layer. The high module fibres is prone to abrasions and shearing effects with the presence of abrasive particles (Fig. 11). Grooves were developed parallel to the motion of the abrasive particles, with a higher depth near the centre and decreases towards the ends. The wear tracks emerge on the contact surface and many abrasive particles accumulated in the composite surface and are pulled out of epoxy matrix as a result of continuous abrasion. The fibres are then sheared and also pulled out in later stages [36]. The unfilled SF-BF/Ep composites shows pulverized matrix, voids, damage of fibre and less matrix masking of fibre was observed (Fig. 11a). High aspect ratio of HNTs gives a large amount of filler to polymer interactions as compared to other nanofillers and hence can be easily dispersed in polymer matrix. HNTs are very well bonded with the matrix which protects the fibre from severe damages (Fig. 11b). Thus, exhibiting a synergistic effect between the HNTs, epoxy and the fibres leading to the enhancement in the abrasion resistance when compared to unfilled SF-BF/Ep composites.

The current research demonstrates that the abrasive wear factors and their corresponding interactions has physical and statistical importance (percentage contribution > error) in wear characteristics of nanocomposites. However, fewer interactions have statistical importance but they are not of physical importance, since the associated error is more than the percentage contributions of both the interactions as indicated in ANOVA results [51].

Table 8. ANOVA table for specific wear rate

Source	DF	Seq SS	Adj SS	Adj MS	F Value	P Value	P (%)
FILLER CONTENT (%)	2	3.285	3.285	1.64249	571.25	0.000	14.13748
LOAD (N)	2	11.5201	11.521	5.76004	2003.31	0.000	49.57846
ABRADING DISTANCE (m)	2	7.672	7.672	3.83598	1334.14	0.000	33.01759
SILICA SAND SIZE (μm)	2	0.6924	0.6924	0.34619	120.4	0.001	2.979846
FILLER CONTENT(%)*LOAD (N)	4	0.0122	0.0122	0.00304	1.06	0.452	0.052505
FILLER CONTENT(%)*ABRADING DISTANCE (m)	4	0.0141	0.0141	0.00352	1.22	0.392	0.060681
FILLER CONTENT(%)*SILICA SAND SIZE	4	0.0232	0.0232	0.00581	2.02	0.21	0.099845
Residual Error	6	0.0173	0.0173	0.00288			0.074453
Total	26	23.2361					100.000

S = 0.05362 R-Sq = 99.9% R-Sq(adj) = 99.7%

3.4 Confirmation Phase

The test for confirmation is indeed the last step in DOE method. Confirmation experiment aims to affirm the conclusions made during its analysis phase [52,53]. Using the aforementioned predictive equation 2 the approximate S/N ratio for the SWR can be determined by the optimum parameter level.

$$\eta_{opt} = U + \sum_{j=1}^{k}(\eta_j - U); \text{ j=1, 2, ...k,} \quad (2)$$

Where, U=Average of all experimental S/N ratio; j=Average of S/N at optimal parameter level; and k=number of major parameters of design that affect significantly the SWR of HNTs filled SF-BF/Ep nanocomposite.

The control factors A_2, B_1, C_3, and D_1, which are not present in the Table 6 DOE, were considered to predict the SN ratio and Ks values, and the respective SWR and SN values were calculated. The findings of experimental validation using optimized wear parameters, as well as comparison of predicted SWR with actual SWR are shown in the Table 9.

Table 9. Confirmation test for SWR.

Level	Optimum process parameter $A_2B_1C_3D_1$ (FillerContent-1.5 Wt. %, Load=20N, Abrading distance= 750m, Silica sand size=225 µm		
	Predicted value	**Experimental value**	**Variation**
S/N ratio (dB)	46.5671	46.5677	0.0006
SWR (mm^3/Nm)	4.695×10^{-3}	4.674×10^{-3}	0.021×10^{-3}

4. CONCLUSION

The tribological characterization of HNTs filled SF-BF/Ep composites was carried out to analyse the potential use of HNTs in hybrid nanocomposites, and the following findings were obtained.

1. The Taguchi method of experimental design allows for the efficient analysis of wear behavior that is affected by various factors like filler content, load, abrading distance and silica sand size.
2. Load has the highest statistical and physical significance among the control factors considered in the three body analysis.
3. Percentage contribution on three-body wear performance of HNTs filled SF-BF-Ep nanocomposite are in following order: Load (P = 49.578%) >>> abrading distance (P = 33.018%) >>> filler content (P = 14.137%) >>> silica sand size (2.9798%)
4. Control factor of A_2, B_1, C_3 and D_1 combination gives the lower SWR.
5. SEM studies of the worn surfaces support the involved mechanisms during the abrasion process. Pulverized matrix, fragmented fibres, voids and fibre damages were observed.
6. HNTs are a promising future material for improving the development of clay-based polymeric composites owing to its low cost and widespread availability. The reinforcement effect of the lower weight fractions of nanofillers was achievable by creating an effective organization of crystalline phases in the HNTs.
7. Finally, HNTs could be viewed as a very viable reinforcing element with significant wear performance improvements for a variety of tribological applications. Therefore, the usage of these HNT filled hybrid nanocomposites may be suggested for applications or places of operation that are abrasive or dusty in nature, such as sieve holders in mining grain tank auger floor liners and elevator buckets.

REFERENCES

[1] D.K. Rajak, D.D. Pagar, P.L. Menezes, E. Linul, *Fiber-reinforced polymer composites: Manufacturing, properties, and applications*, Polymers, vol. 11, iss. 10, pp. 1-37, 2019, doi: 10.3390/polym11101667

[2] M.Ö. Seydibeyoğlu, A.K. Mohanty, M. Misra, *Fiber Technology for Fiber-Reinforced Composites*, Elsevier, 2017.

[3] M.F. Ashby, Y.J.M. Bréchet, *Designing hybrid materials,* Acta Materialia, vol. 51, iss. 19, pp. 5801–5821, 2003, doi: 10.1016/S1359-6454(03)00441-5

[4] M.T. Dehkordi, H.Nosraty, M.M. Shokrieh, G. Minak, D. Ghelli, *Low velocity impact properties of intra-ply hybrid composites based on basalt and nylon woven fabrics,* Materials and Design, vol. 31, iss. 8, pp. 3835–3844, 2010, doi: 10.1016/j.matdes.2010.03.033

[5] F. Kundie, C.H. Azhari, A. Muchtar, Z.A. Ahmad, *Effects of filler size on the mechanical properties of polymer-filled dental composites: A review of recent developments*, Journal of Physical Science, vol. 29, no. 1, pp. 141–165, 2018, doi: 10.21315/jps2018.29.1.10

[6] I. Hutchings, P. Shipway, *Tribology: Friction and wear of engineering materials*: Second Edition, Elsevier, 2017.

[7] A. Lotfi, H. Li, D.V. Dao, G. Prusty, *Natural fiber–reinforced composites: A review on material, manufacturing, and machinability,* Journal of Thermoplastic Composite Materials, vol. 34, iss. 2. pp. 238–284, 2021, doi: 10.1177/0892705719844546

[8] C.J. Zhou, Y. Li, S.W. Yao, J. H. He, *Silkworm-based silk fibers by electrospinning,* Results in Physics, vol. 15, Available online, 2019, doi: 10.1016/j.rinp.2019.102646

[9] S.M. Darshan, B. Suresha, G.S. Divya, *Waste Silk Fiber Reinforced Polymer Matrix Composites: A Review*, Indian Journal of Advances in Chemical Science, vol. S1, pp. 183–189, 2016.

[10] G.B. Manjunatha, K.N. Bharath, *Fracture Analysis on Silk and Glass Fiber-Reinforced Hybrid Composites*, in A. Khan, S.M. Rangappa, M. Jawaid, S. Siengchin, A.M. Asiri (Ed.): Hybrid Fiber Composites, Wiley, pp. 87–97, 2020, doi: 10.1002/9783527824571.ch5

[11] S.M. Darshan, B. Suresha, *Effect of basalt fiber hybridization on mechanical properties of silk fiber reinforced epoxy composites,* Materials Today: Proceedings, vol. 43, 2021, pp. 986–994, doi: 10.1016/j.matpr.2020.07.618

[12] I. Van de Weyenberg, J. Ivens, A. De Coster, B. Kino, E. Baetens, I. Verpoest, *Influence of processing and chemical treatment of flax fibres on their composites,* Composites Science and Technology, vol. 63, iss. 9, pp. 1241–1246, 2003, doi: 10.1016/S0266-3538(03)00093-9

[13] S. Khandelwal, K.Y. Rhee, *Recent advances in basalt-fiber-reinforced composites: Tailoring the fiber-matrix interface,* Composites Part B: Engineering, vol. 192, Available online, 2020, doi: 10.1016/j.compositesb.2020.108011

[14] J.M. Park, W.G. Shin, D.J. Yoon, *A study of interfacial aspects of epoxy-based composites reinforced with dual basalt and SiC fibres by means of the fragmentation and acoustic emission techniques,* Composites Science and Technology, vol. 59, iss. 3, pp. 355–370, 1999, doi: 10.1016/S0266-3538(98)00085-2

[15] A. Kausar, *Review on Polymer/Halloysite Nanotube Nanocomposite,* Polymer - Plastics Technology and Engineering, vol. 57, iss. 6, pp. 548–564, 2018, doi: 10.1080/03602559.2017.1329436

[16] H. Dodiuk, S.H. Goodman, *Handbook of Thermoset Plastics*, Elsevier, 2013, doi: 10.1016/C2011-0-09694-1

[17] C.R. Raajeshkrishna, P. Chandramohan, A. Babatunde Obadele, *Friction and thermo mechanical characterization of nano basalt reinforced epoxy composites,* International Journal of Polymer Analysis and Characterization, vol. 26, iss. 5, pp. 425–439, 2021, doi: 10.1080/1023666X.2021.1899692

[18] O. Zabihi, M. Ahmadi, S. Nikafshar, K. Chandrakumar Preyeswary, M. Naebe, *A technical review on epoxy-clay nanocomposites: Structure, properties, and their applications in fiber reinforced composites*, Composites Part B: Engineering, vol. 135, pp. 1–24, 2018, doi: 10.1016/j.compositesb.2017.09.066

[19] C. Dong, *Review of natural fibre-reinforced hybrid composites,* Journal of Reinforced Plastics and Composites, vol. 37, iss. 5, pp. 331–348, 2018, doi: 10.1177/0731684417745368

[20] D.K.K. Cavalcanti, M.D. Banea, J.S.S. Neto, R.A.A. Lima, L.F.M. da Silva, R.J.C. Carbas, *Mechanical characterization of intralaminar natural fibre-reinforced hybrid composites*, Composites Part B: Engineering, vol. 175, 2019, doi: 10.1016/j.compositesb.2019.107149

[21] H. Czichos, T. Saito, L. Smith, *Springer Handbook of Metrology and Testing*, Springer, 2011.

[22] K. Friedrich, *Polymer composites for tribological applications,* Advanced Industrial and Engineering Polymer Research, vol. 1, iss. 1, pp. 3–39, 2018, doi: 10.1016/j.aiepr.2018.05.001

[23] Y. Şahin, H. Şahin, *Microstructure and Abrasive Wear of Particle-Filled Composites*, in Lecture Notes in Mechanical Engineering, Springer, 2021, pp. 623–634, doi: 10.1007/978-981-15-9893-7_46

[24] Y. Şahin, A. Deniz, F. Şahin, *Investigation of abrasive wear performances of different polyamides by response surface methodology*, Tribology in Industry, vol. 41, no. 3, pp. 321–329, 2019, doi: 10.24874/ti.2019.41.03.02

[25] B.F. Yousif, S.T.W. Lau, S. McWilliam, *Polyester composite based on betelnut fibre for tribological applications,* Tribology International, vol. 43, iss. 1–2, pp. 503–511, 2010, doi: 10.1016/j.triboint.2009.08.006

[26] L. Chang, Z. Zhang, C. Breidt, K. Friedrich, *Tribological properties of epoxy nanocomposites I. Enhancement of the wear resistance by nano-TiO_2 particles, Wear*, vol. 258, iss. 1-4, pp. 141–148, 2005, doi: 10.1016/j.wear.2004.09.005

[27] S.R. Lu, J. Hongyu, H.L. Zhang, X. Y. Wang, *Wear and mechanical properties of epoxy/SiO2-TiO2 composites,* Journal of Materials Science, vol. 40, iss. 11, pp. 2815–2821, 2005, doi: 10.1007/s10853-005-2437-2

[28] B.M. Rudresh, B.N. Ravikumar, D. Madhu, B.V. Lingesh, *Three body abrasive wear behavior of glass-basalt PA66/PTFE hybrid composites in multi pass condition,* Tribology in Industry, vol. 41, no. 3, pp. 416–425, 2019, doi: 10.24874/ti.2019.41.03.11

[29] Y. Şahin, F. Şahin, *Effects of process factors on tribological behaviour of epoxy composites including Al_2O_3 nano particles: a comparative study on multi-regression analysis and artificial neural network,* Advances in Materials and Processing Technologies, Published online, 2021, doi: 10.1080/2374068X.2021.1878712

[30] C.R. Mahesha, Shivarudraiah, N. Mohan, R. Suprabha, *Three Body Abrasive Wear Studies on Nanoclay/NanoTiO_2 filled Basalt-Epoxy Composites*, *in Materials Today: Proceedings*, vol. 4, iss. 2, pp. 3979–3986, 2017, doi: 10.1016/j.matpr.2017.02.298

[31] A. Patnaik, A, Satapathy, S. Biswas, *Investigations on Three-Body Abrasive Wear and Mechanical Properties of Particulate Filled Glass Epoxy Composites,* Malaysian Polymer Journal, vol. 5, no. 2, pp. 37-48, 2010.

[32] R. Namdeo, S. Tiwari, and S. Manepatil, *Optimization of High Stress Abrasive Wear of Polymer Blend Ethylene and Vinyl Acetate Copolymer/HDPE/MA-g-PE/OMMT Nanocomposites*, Journal of Tribology, vol. 139, iss. 2, 2017, doi: 10.1115/1.4034696

[33] V. Sharma, M.L. Meena, M. Kumar, A. Patnaik, *Mechanical and three-body abrasive wear behavior analysis of glass and basalt fiber-reinforced epoxy composites,* Polymer Composites, vol. 41, iss. 9, pp. 3717–3731, 2020, doi: 10.1002/pc.25670

[34] S.M. Vinu Kumar, B. Suresha, G. Rajamurugan, A. Megalingam, *Mechanical and abrasive wear behavior of cenosphere filled carbon reinforced epoxy composites using Taguchi-Grey relational analysis*, Materials Research Express, vol. 6, iss. 1, 2019, doi: 10.1088/2053-1591/aae5dc

[35] B. Suresha, G. Chandramohan, *Three-body abrasive wear behaviour of particulate-filled glass-vinyl ester composites,* Journal of Materials Processing Technology, vol. 200, iss. 1-3, 2008, doi: 10.1016/j.jmatprotec.2007.09.035

[36] B. Muralidhara, S.P. Kumaresh Babu, G. Hemanth, B. Suresha, *Optimization of abrasive wear behaviour of halloysite nanotubes filled carbon fabric reinforced epoxy hybrid composites,* Surface Topography: Metrology and Properties, vol. 8, iss. 4, 2020, doi: 10.1088/2051-672X/abc8e1

[37] M. Sakthivel, K. Srinivasan, A.G. Ganesh Kumar, *Wear behavior of sansevieria cylindrica and E-glass reinforced polyester composites*, Materialpruefung/Materials Testing, vol. 61, iss. 3, pp. 239–242, 2019, doi: 10.3139/120.111310

[38] K.M. Subbaya, N. Rajendra, Y.S. Varadarajan, B. Suresha, *Multiple Response Optimization of Three-Body Abrasive Wear Behaviour of Graphite Filled Carbon-Epoxy ComPosites Using Grey-Based Taguchi Approach,* Journal of Minerals and Materials Characterization and Engineering, vol. 11, no. 09, pp. 876–884, 2012, doi: 10.4236/jmmce.2012.119082

[39] B.N. Ramesh, B. Suresha, *Optimization of tribological parameters in abrasive wear mode of carbon-epoxy hybrid composites,* Materials and Design, vol. 59, pp. 38–49, 2014, doi: 10.1016/j.matdes.2014.02.023

[40] N. Sapiai, A. Jumahat, M. Jawaid, C. Santulli, *Abrasive wear behavior of CNT-filled unidirectional kenaf-epoxy composites*, Processes, vol. 9, iss. 1, pp. 1–15, 2021, doi: 10.3390/pr9010128

[41] G. Taguchi, S. Konishi, *Taguchi methods, orthogonal arrays and linear graphs: Tools for quality engineering*, American supplier institute, 1987.

[42] M. Arulra, P.K. Palani, L. Venkatesh, *Optimization of Process Parameters in Stir Casting of Hybrid Metal Matrix (LM25/SiC/B4C) Composite Using Taguchi Method,* Journal of Advances in Chemistry, vol. 13, no. 11, pp. 6038–6042, 2017, doi: 10.24297/jac.v13i11.5774

[43] Y. Yang, D. Zhao, J. Xu, Y. Dong, Y. Ma, X. Qin, K. Fujiwara, E. Suzuki, T. Furukawa, Y. Takai, H. Hamada, *Mechanical and optical properties of silk fabric/glass fiber mat composites: an artistic application of composites,* Textile Research Journal, vol. 88, iss. 8, pp. 932–945, 2018, doi: 10.1177/0040517517690621

[44] J. Bijwe, J. Indumathi, A.K. Ghosh, *Influence of weave of glass fabric on the oscillating wear performance of polyetherimide (PEI) composites,* Wear, vol. 253, iss. 7–8, pp. 803–812, 2002, doi: 10.1016/S0043-1648(02)00167-9

[45] M. Arulraj, P.K. Palani, M. Sowrirajan, S. Vijayan, J. P. Davim, *Optimization and effect of squeeze casting process parameters on tensile strength of hybrid metal matrix composite,* Journal of Manufacturing Technology Research, vol. 11, iss. 3–4, pp. 137–154, 2019.

[46] K.M. Subbaya, B. Suresha, N. Rajendra, Y.S. Varadarajan, *Taguchi approach for characterization of three-body abrasive wear of carbon-epoxy composite with and without SiC filler*, Composite Interfaces, vol. 19, iss. 5, pp. 297–311, 2012, doi: 10.1080/15685543.2012.720903

[47] C.Z. Liu, L.Q. Ren, J. Tong, T.J. Joyce, S.M. Green, R.D. Arnell, *Statistical wear analysis of PA-6/UHMWPE alloy, UHMPE and PA-6,* Wear, vol. 249, iss. 1–2, pp. 31–36, 2001, doi: 10.1016/S0043-1648(00)00555-X

[48] C.J. Schwartz, S. Bahadur, *The role of filler deformability, filler-polymer bonding, and counterface material on the tribological behavior of polyphenylene sulfide (PPS),* Wear, vol. 251, no. 1-12, pp. 1532–1540, 2001, doi: 10.1016/S0043-1648(01)00799-2

[49] H. Rajashekaraiah, S. Mohan, P.K. Pallathadka, S. Bhimappa, *Dynamic mechanical analysis and three-body abrasive wear behaviour of thermoplastic copolyester elastomer composites,* Advances in Tribology, vol. 2014, 2014, doi: 10.1155/2014/210187

[50] S. Basavarajappa, A.G. Joshi, K.V. Arun, A.P. Kumar, M.P. Kumar, *Three-body abrasive wear behaviour of polymer matrix composites filled with SiC particles,* Polymer - Plastics Technology and Engineering, vol. 49, iss. 1, pp. 8–12, 2010, doi: 10.1080/03602550903206407

[51] S.R. Chauhan, A. Kumar, I. Singh, P. Kumar, *Effect of Fly Ash Content on Friction and Dry Sliding Wear Behavior of Glass Fiber Reinforced Polymer Composites - A Taguchi Approach*, Journal of Minerals and Materials Characterization and Engineering, vol. 9, no. 04, pp. 365–387, 2010, doi: 10.4236/jmmce.2010.94027

[52] E.R. Ziegel, P. Ross, *Taguchi Techniques for Quality Engineering,* Technometrics, vol. 39, iss. 1, pp. 109-110, 1997, doi: 10.2307/1270793

[53] B. Suresha, R.S. Shenoy, R. Bhat, P.K. Sohan, R. Hemanth, *Optimization of wear behaviour of boron nitride filled polyaryletherketone composites by Taguchi approach,* Materials Research Express, vol. 6, iss. 8, 2019, doi: 10.1088/2053-1591/ab23e5